P2.44 A NEW PARAMETRIC TROPICAL CYCLONE PRESSURE-WIND PROFILE MODEL

Vincent T. Wood[1], Luther W. White[2], David P. Jorgensen[1], and Hugh E.Willoughby[3]
[1]NOAA/OAR/National Severe Storms Laboratory, Norman, OK
[2]Department of Mathematics, University of Oklahoma, Norman, OK
[3]Department of Earth and Environment, Florida International University, Miami, FL

1. INTRODUCTION

Intense tropical cyclones have been observed to exhibit multiple, well-defined wind maxima during an eye replacement cycle (Willoughby et al. 1982). Two concentric eyewalls were defined by two tangential wind peaks in each of the aircraft radial legs and by two well-defined rings of enhanced radar reflectivity located at different radii from the tropical cyclone centers. An echo-free moat and a saddle-shaped wind profile were situated between the concentric eyewalls. The eyewall replacement cycle (ERC) occurs when replacement of the inner eyewall by the outer eyewall coincides with a decrease in storm intensity (Willoughby et al. 1982; Willoughby 1990a; Black and Willoughby 1992; Sitkowski et al. 2011). The cycle is often accompanied by significant fluctuations (i.e., initial weakening followed by reintensification) in maximum wind speed and central surface pressure of the storm.

The objective of this paper is to develop a new parametric tropical cyclone pressure-wind profile model for accurately depicting surface pressure profiles corresponding to the complex tropical cyclone wind profiles that exhibit single- and dual-maximum concentric-eyewall tangential wind peaks. The Wood and White (2011) model employs the five key parameters that control the radial profile of tangential wind: maximum tangential velocity, radius of maximum tangential wind, and three shape parameters that independently control different portions of the velocity profiles. Furthermore, the model uses a cyclostrophic-balance wind equation to employ a partitioning of the total surface pressures into separate pressure components that, respectively, correspond to a primary and secondary cyclostrophic tangential wind profiles. The partitioning scheme aids investigators to quantitatively evaluate and interpret the significant fluctuations in central surface pressure deficits and gradient wind maxima during an ERC.

2. PARAMETRIC MODELING OF TROPICAL CYCLONE PRESSURE-WIND PROFILES

2.1 Partitioned wind profiles for two peak tangential wind profiles

The dual concentric eyewall structure can be considered as a dual vortex composed of the inner and outer vortex configurations. We now show that the hypothesis on a two-vortex composite in a tropical cyclone wind profiles enables the description of complex tangential velocity distributions. To quantitatively describe the complex tangential velocity distributions in this structure, we isolate one primary (inner eyewall) tangential wind profile from the secondary (outer eyewall) tangential wind profile by partitioning a total cyclostrophic wind (V_c) profile into the primary (V_p) and secondary (V_s) tangential wind profiles. They are given as

$$V_c = V_p + V_s , \tag{1}$$

where the partitioned tangential wind components in (1) are expressed by

$$V_p = \frac{V_{x\_p}\phi_p}{2}\left(R_{cx\_p}^{-1} + 2\sqrt{1+\frac{1}{4}R_{cx\_p}^{-2}} \right), \tag{2a}$$

$$R_{cx\_p} = \frac{V_{x\_p}}{f R_{x\_p}}, \phi_p = \frac{\eta^{\lambda_p}\rho_p^{\kappa_p}}{\left(\eta_p - \kappa_p + \kappa_p \rho^{\eta_p/\lambda_p}\right)^{\lambda_p}}, \tag{2b}$$

$$V_s = \frac{V_{x\_s}\phi_s}{2}\left(R_{cx\_s}^{-1} + 2\sqrt{1+\frac{1}{4}R_{cx\_s}^{-2}} \right), \tag{3a}$$

$$R_{cx\_s} = \frac{V_{x\_s}}{f R_{x\_s}}, \phi_s = \frac{\eta^{\lambda_s}\rho_s^{\kappa_s}}{\left(\eta_s - \kappa_s + \kappa_s \rho^{\eta_s/\lambda_s}\right)^{\lambda_s}}. \tag{3b}$$

Here, the parenthesis on the right-hand sides of (2a) and (3a) represents the scaled cyclostrophic tangential wind approximation formulated in terms of a local cyclostrophic Rossby number, following Willoughby (1990a, 1995, 2011). V_{x_p} and V_{x_s} are maximum tangential winds associated with the inner and outer concentric eyewalls, respectively. R_{cx_p} and R_{cx_s} are local cyclostrophic Rossby numbers based on the characteristic tangential wind maxima (V_{x_p}, V_{x_s}) at their characteristic radii (R_{x_p}, R_{x_s}), and f is the Coriolis parameter. The variables $\rho_p \equiv r / R_{x\_p}$ and $\rho_s \equiv r / R_{x\_s}$ are dimensionless radii from a tropical cyclone center. ϕ_p and ϕ_s, respectively, are the dimensionless functions that construct the primary and secondary tangential wind profiles in which three shape velocity parameters (κ, η and λ) each control different portions of the profile, as formulated by Wood and White (2011). The roles of these parameters in the physical behavior of the radial profile families of tangential velocity are described in detail in the Wood and White article.

In (1), the primary eyewall wind component (V_p) is the primary tangential wind in a basic-state vortex flow.

Corresponding author address: Vincent T. Wood, National Severe Storms Laboratory, 120 David L. Boren Blvd., Norman, OK 73072. E-mail: Vincent.Wood@noaa.gov

The secondary tangential wind (V_s) perturbation added to the primary vortex is the perturbation that forms a double-peaked tangential wind profile when it is imposed on the basic state (e.g., Schubert et al. 1980). Using (1), the cyclostrophic wind balance for an axisymmetric tropical cyclone is employed to derive a single pressure profile from the complex tangential wind profile, and will be presented in the subsequent subsection.

To tailor the Wood-White parametric wind model for tropical cyclone applications, we follow Willoughby (1990b, 1995, 2011) and use the fact that a gradient wind (V_g) is computed from the cyclostrophic wind (V_c) approximation formulated in terms of the cyclostrophic Rossby number [$R_c = V_c/(fr)$], given by

$$V_g = \frac{V_c}{\frac{1}{2}\left(R_c^{-1} + 2\sqrt{1+\frac{1}{4}R_c^{-2}}\right)}, \quad R_c \neq 0 . \qquad (4)$$

Here, we have chosen the positive root in the denominator of (4) in order to model non-anomalous flow around a low-pressure system. The terms in the parenthesis on the right-hand side of (2a) and (3a) are needed to increase the cyclostrophic wind so that when it is used to compute the gradient wind in (4), the value comes out right. Using (1), the cyclostrophic wind balance for an axisymmetric tropical cyclone is employed to derive a single pressure profile from the complex wind profile, and will be presented in the subsequent subsection.

2.2 Cyclostrophic wind balance

Apart from low-altitude supergradient winds, the relationship between tangential winds and pressures in tropical cyclones is well represented using the gradient-wind approximation (Willoughby 1990a,b, 1991, 2011). Eq. (4) is easier to compute a gradient wind from the available model cyclostrophic wind in (1) than from a gradient-wind balance equation. This is because the radial integral of the Coriolis term (fV_g) in the gradient-wind relationship is not bounded at infinity. To avoid this difficulty, it is best to use the simple cyclostrophic wind relationship without the Coriolis term with an accepted level of accuracy. That is, we set up a cyclostrophic wind such that when the gradient wind formula is applied, the observed wind profile is well recovered. The resulting profile is in gradient balance so that we are not using the cyclostrophic approximation to represent the wind. Cast in terms of geopotential height (Z) of an isobaric surface instead of surface pressure (e.g., Willoughby and Rahn 2004), the cyclostrophic wind relationship is given by

$$\frac{V_c^2}{r} = g\frac{\partial Z}{\partial r}, \qquad (5)$$

where g is the acceleration of gravity. It is convenient and simple to compute both the gradient wind (4) and the geopotential height (5) from the cyclostrophic wind. The gradient wind will drop off more quickly with radius in the part of the domain where $R_c \ll 1$; however, having radial integrals that are readily bounded at infinity and a more rapid decrease in V_g in the unsampled part of the domain at large radius more than compensate for that difficulty.

The geopotential height $Z(r)$ is obtained by integrating (5) radially inward from an environmental geopotential height (Z_e), and is given by

$$Z(r) = Z_e + \frac{1}{g}\int_{\infty}^{r}\frac{V_c^2(r')}{r'}dr', \qquad (6)$$

where $Z_e\,[= Z(r \to \infty)]$ is the environmental (undisturbed) geopotential height at infinitely far from the tropical cyclone center, and r' is a dummy variable for the integration, which is done numerically. (6) is extrapolated from the aircraft flight level to the surface (at a nominal height of 10 m) under the assumption of the mean temperature $\overline{T} = (T_{ss} + T_{fl})/2$ of a tropical atmospheric layer between the flight level (subscript fl) and the sea surface (ss), where $T_{ss} = 300$ K is the typical temperature at the sea surface and T_{fl} is the temperature at the flight level. Assuming that $\overline{T}$ is independent of r and substituting (6) into the hypsometric equation yield the surface pressure P_{sfc} within the tropical cyclone region

$$P_{sfc}(r) = P_e \exp\left(\frac{1}{R_d\overline{T}}\int_{\infty}^{r}\frac{V_c^2(r')}{r'}dr'\right), \qquad (7)$$

where $P_e = P_{fl}\exp[gZ_e/(R_d\overline{T})]$. Here, P_{fl} is the pressure altitude at the flight level outside the tropical cyclone region, R_d is the gas constant for dry air, and P_e is the asymptotic environmental surface pressure that is extrapolated from Z_e in the environmental tropical atmosphere. (7) contains the pressure-adjusted flight-level tangential winds but is extrapolated to the pressure at the sea surface. In this study, the Z_e values of 850 hPa and 700 hPa in the standard atmosphere (U.S. Standard Atmosphere 1976) are, respectively, 1457 m and 3012 m. Inward radial integration of (7) requires a known environmental pressure (P_e) at the sea surface and at a large radius where a zero asymptotic cyclostrophic wind (0.001 m s^{-1} in this study) occurs. Since P_e is chosen to be the mean value of 1014.3 hPa based on their climatological analyses of Knaff and Zehr (2007), the calculated values of $\overline{T}$, respectively, are found to be 278 K and 282 K for the mean temperature of the standard 700- and 850-hPa layers at Z_e. Furthermore, (7) involves an integral which is calculated using the trapezoidal rule (e.g., Press et al. 1992, p. 125-126).

2.3 Partitioned pressure profiles for two peak tangential wind profiles

In the cyclostrophic wind relationship, a total surface pressure (P_{tot}) corresponds to the radial profiles of the total (summed) cyclostrophic winds and is obtained by incorporating (1) into (7). As a consequence, $P_{sfc}(\equiv P_{tot})$ is partitioned into two different pressure components that correspond to the individual radial profiles of V_p and V_s, respectively,

$$P_{sfc}(r) \equiv P_{tot}(r) = \frac{P_p(r)P_s(r)}{P_e}, \quad (8)$$

where the partitioned surface pressure components are expressed by

$$P_p(r) = P_e \exp\left[\frac{1}{R_d\overline{T}}\int_{\infty}^{r}\left(\frac{V_p^2(r')+V_p(r')V_s(r')}{r'}\right)dr'\right], \quad (9)$$

and

$$P_s(r) = P_e \exp\left[\frac{1}{R_d\overline{T}}\int_{\infty}^{r}\left(\frac{V_s^2(r')+V_s(r')V_p(r')}{r'}\right)dr'\right]. \quad (10)$$

Note in (9)-(10) that $P_e\,[=P(r\to\infty)]$ is the extrapolated environmental surface pressure at which the winds decrease asymptotically to zero infinitely far from the tropical cyclone center. On the right-hand side of (9), V_p^2 contributes most to the primary surface pressure (P_p). The product of V_p and V_s partially contributes to P_p only if there is a secondary wind maximum ($V_{x\_s}\neq 0$) in the radial profile of V_s. On the right-hand side of (10), V_s^2 mainly contributes to the secondary surface pressure (P_s), while the product of V_sV_p plays a minor role in modulating the radial profile of P_s. As will be shown in the later sections, the relative contributions of V_p and V_s to the total surface pressure (P_{sfc}) will be explored and compared to elucidate the role of the partitioned tangential wind profiles in the physical behavior of the corresponding surface pressure profiles and surface pressure deficits at the storm center.

2.4 Partitioned central surface pressure deficits for two peak tangential wind profiles

In order to obtain a total central surface pressure deficit (ΔP_{sfc}) that corresponds to two individual tangential wind profile components (V_p and V_s), (8) is differentiated with respect to r such that

$$\frac{\partial P_{sfc}}{\partial r} \equiv \frac{\partial P_{tot}}{\partial r} = \frac{P_s}{P_e}\frac{\partial P_p}{\partial r} + \frac{P_p}{P_e}\frac{\partial P_s}{\partial r}, \quad (11)$$

where the partitioned radial surface pressure gradient components are given by

$$\frac{\partial P_p}{\partial r} = \frac{P_p}{R_d\overline{T}}\left(\frac{V_p^2+V_pV_s}{r}\right), \quad (12)$$

and

$$\frac{\partial P_s}{\partial r} = \frac{P_s}{R_d\overline{T}}\left(\frac{V_s^2+V_sV_p}{r}\right). \quad (13)$$

The total central surface pressure deficit (ΔP_{sfc}) at the storm center thus is obtained by integrating (11) inward from P_e, thereby yielding

$$\Delta P_{sfc}(r) \equiv \Delta P_{tot}(r) = \Delta P_p(r) + \Delta P_s(r), \quad (14)$$

where the partitioned radial surface pressure deficit components are expressed by

$$\Delta P_p(r) = \frac{1}{P_e}\int_{\infty}^{0} P_s(r')\frac{\partial P_p(r')}{\partial r'}dr' < 0, \quad (15)$$

and

$$\Delta P_s(r) = \frac{1}{P_e}\int_{\infty}^{0} P_p(r')\frac{\partial P_s(r')}{\partial r'}dr' < 0. \quad (16)$$

As will be presented in the subsequent section, (14)-(16) are useful in diagnosing and evaluating the significant fluctuations in central surface pressure deficits and cyclostrophic/gradient wind maxima that correspond to the primary and secondary concentric eyewalls during the ERC.

3. TROPICAL CYCLONE EMULATOR

This section uses a tropical cyclone emulator to investigate the effects of the single- and dual-maximum eyewall tangential winds on the behavior of central surface pressure deficits and radial profiles of surface pressure and cyclostrophic Rossby number in varying stages of tropical cyclone development from a hurricane (< 50 m s^{-1}) with its single-maximum tangential wind profile to a major hurricane (> 50 m s^{-1}) with its dual-maximum tangential wind profile. We performed different model parameters by varying at least one of any model parameters ($\mathbf{m}=[V_X, R_X, \kappa, \eta, \lambda]^{\mathrm{T}}$). Table 1 lists the selected parameter values used for the four experiments.

Following is an overview of assumptions made for the emulator. In order to simulate an idealized tropical cyclone, we followed Willoughby (1990a,b; 1991; 2011) who found from numerous aircraft measurements that the gradient wind balance was a good approximation to the azimuthally averaged tangential winds in most portions of an inner eyewall above a boundary layer where the strong radial inflows cannot be negligible in intense tropical cyclones. The NOAA's Atlantic Oceanographic and Meteorological Laboratory's Hurricane Research Division flight-level data archive (Willoughby and Rahn, 2004) provided consistent wind and geopotential height observations in hurricanes as functions of azimuth and time at fixed pressures. By averaging over azimuth and allowing for linear variation of the wind and geopotential height at fixed radii with time, these data provided an accurate depiction of the time-varying azimuthally symmetric structure at a single level over 4-6 h (Willoughby 1990a,b). The maximum of the mean wind and its radius determined in this fashion were consistent estimates of *RMW* (radius of maximum wind) and V_X. They also have the advantage of being close to gradient balance except (as in the boundary

layer under the eyewall) where azimuthal mean accelerations were large. It is important to recognize that the maximum azimuthally averaged wind and its radius were different from the average maximum wind and the average radius of maximum wind (i.e., mature tropical cyclones are rarely truly symmetric over their lifetimes).

The individual profiles that made up the mean varied from it in interesting ways. They were generally not in gradient balance and many (if not most) of the individual profile wind maxima were stronger than the azimuthal mean maximum, but at different radii. The mean-wind profile was generally broader than the profiles that composed it because these maxima fell at different radii. Many (but not all) of the supergradient winds reported in the tropical cyclone literature appeared as the results of asymmetric radial accelerations (Kepert 2001; Kepert and Wang 2001) when analyzed in this way. A key strength of this analysis was that the variations among the observed profiles can be treated as perturbations (non-necessarily linear) on a well behaved, nearly balanced mean vortex.

Since a translation movement of the tropical cyclone was not taken into account in the model, the model tropical cyclone was assumed to be stationary in a quiescent, tropical environment (i.e., no external influences such as upwelling of cold water on the wind profile). The cyclone was assumed to be positioned at 20° latitude in this study.

3.1 Hurricanes with single- vs. dual-maximum tangential winds

Figure 1 illustrates a change of a tropical cyclone structure of tangential wind and surface pressure profiles when a single-maximum concentric-eyewall tangential wind profile evolves to a developing dual-maximum concentric-eyewall tangential wind profile. To initialize the single-maximum tangential wind profile in a model mature hurricane A, we used the wind model parameters in Table 1, and set V_{x_s} equal to zero in (3a) so that (1)-(16) were reduced to the form:

$$V_c = V_p\,, \tag{17}$$

$$P_{sfc}(r) = P_p(r) = P_e \exp\left[\frac{1}{R_d \overline{T}}\int_{\infty}^{r}\frac{V_p^2(r')}{r'}dr'\right], \tag{18}$$

$$\frac{\partial P_{sfc}}{\partial r} = \frac{\partial P_p}{\partial r} = \frac{P_p}{R_d \overline{T}}\left(\frac{V_p^2}{r}\right), \tag{19}$$

and $$\Delta P_{sfc}(r) = \Delta P_p(r) = \int_{\infty}^{0}\frac{\partial P_p(r')}{\partial r'}dr' < 0\,. \tag{20}$$

Because $V_{x\_s} = 0$, we set $P_s / P_e = 1$ in (11) and (15) which yields (19) and (20). Using the available cyclostrophic wind ($V_c = V_p$) profile, V_g readily is calculated from (4). Fig. 1 shows the radial profiles of primary cyclostrophic and gradient winds, cyclostrophic Rossby number (R_c), surface pressure (P_{sfc}) and central surface pressure deficit (ΔP_{sfc}) in the model hurricane A. One rationale for presenting the side-by-side panels in the figure is to compare the impact of changing one or more model parameters on the two hurricanes' radial profiles of V_c, V_g, R_c, P_{sfc}, and ΔP_{sfc}.

Prior to the formation of a secondary concentric eyewall, the model hurricane A exhibits its single-maximum tangential wind (Fig. 1a). A new outer eyewall in response to convective heat release (Willoughby et al. 1982) induces a new secondary tangential wind (V_s) perturbation, while the developing eyewall migrates slowly inward in the model hurricane B (Fig. 1b). Addition of the V_s profile to the pre-existing profile of the primary tangential wind (V_p) results in a significant change in the V_c and V_g profiles and thus the wind minimum in the saddle-shaped profile.

The radial variations of $P_{sfc}(\equiv P_{tot})$ and $\Delta P_{sfc}(\equiv \Delta P_{tot})$ correspond to the varying profiles of V_c when a single-maximum tangential wind transitions to a dual-maximum tangential wind (Figs. 1c,d). It is noteworthy that, prior to the inception of the secondary eyewall, the P_p profile (gray curve in Fig. 1d) in hurricane B is identical to that profile (black curve in Fig. 1c) in hurricane A. The most significant feature in Fig. 1d is that, after the formation of the V_s profile (Fig. 1b), the radial distribution of P_p in hurricane B has fallen considerably (a gray downward-pointing arrow connecting the gray curve to the black short-dashed curve in Fig. 1d). This is largely because the nonzero V_s profile in the product of V_p and V_s [see Eq. (9), for example] partially contributes to P_p, while V_p remains unchanged in both hurricanes A and B. In this situation, the P_p drop is approximately -11 hPa at the storm center.

The radial profile of zero V_s is flat inside *r* = 35 km (long-dashed curve in Fig. 1b) and causes the P_s profile to become flat between *r* = 0 and *r* = 70 km. The product of P_p, P_s and P_e computed from (8), via (9) and (10), changes the radial distribution of P_{tot} (black solid curve). This product causes the central surface pressure to plummet from 967 hPa in hurricane A to 915 hPa in hurricane B, although V_{x_p} and R_{x_p} in both hurricanes are assumed to be unvaried. Furthermore, the central surface pressure deficits are $\Delta P_{sfc}(\equiv \Delta P_{tot})$ = -47 and -99 hPa in the respective hurricanes.

An important feature of the P_{tot} profile in Fig. 1d is the appearance of a slight "dip" or "kink" at approximately *r* = 80 km (as indicated by a black arrow pointing upward). The P_s profile corresponding to the V_s profile remains flat with radius from the storm center to approximately 70 km, where the profile imperceptibly

begins to increase slowly with radius. Thus, the weak "dip" in the P_{tot} profile results from (8) at approximately 80 km from the storm center. There is a striking similarity between the radial profiles of V_g and P_{sfc} and also of the flight-level tangential wind and 700-hPa geopotential height observed by aircraft in Hurricane Allen (1980), as shown in their Fig. 15 of Willoughby et al. (1982). Furthermore, the V_g and P_{sfc} profiles compare favorably with the flight-level tangential wind and surface pressure profiles calculated (via the gradient-wind balance equation) from aircraft observations of Hurricane Hugo (1989) in Fig. 15 of Marks et al. (2008).

3.2 Major hurricanes with dual-maximum tangential winds undergoing an ERC

Figure 2 presents an ERC when replacement of the inner eyewall by the outer eyewall coincides with a decrease in storm intensity. To model the changes in the tangential wind and surface pressure profiles of intensifying tropical cyclones undergoing the ERC, hurricanes C and D (Table 1) were simulated.

The evolution of the wind profiles from hurricane C to hurricane D is illustrated in the top panels of Fig. 2. As the hurricane D's secondary eyewall becomes fully developed, the primary tangential wind maximum (V_{x_p}) collapses and the primary wind (V_p) decreases asymptotically to zero with radius from the eye with time (Fig. 2b). This wind change causes $P_{sfc}(\equiv P_{tot})$ to rise from 912 hPa (Fig. 2c) to 942 hPa (Fig. 2d) within the eye, thereby reducing the total central surface pressure deficit (ΔP_{tot}). The central surface pressure increases only when the P_p rise due to the weakening of the inner eyewall exceeds the P_s fall due to the strengthening of the outer eyewall (Willoughby et al. 1982). Additionally, the already strong V_s increases further and the wind maximum (V_{x_s}) slowly contracts toward the storm center, thereby deepening the P_s fall in order to keep the P_{tot} from further rising (not shown).

When the inner eyewall disintegrates, the V_p profile diminishes, and the P_p profile returns to the environmental P_e profile, yielding $\Delta P_p = 0$ (not shown). Consequently, the storm weakens a short period of time. Concurrently, the old V_s profile associated with the old outer eyewall now becomes the new V_p profile associated with the new inner eyewall (not shown). The collapse of the old inner eyewall results in an enlarged hurricane (i.e., with a wider primary eyewall).

When the secondary wind maximum intensity surpasses the primary wind maximum intensity, the storm begins to re-intensify in tandem with the new P_p fall. When the old primary wind maximum no longer exists, the ERC is complete, and the storm reverts to a single concentric eyewall structure. The entire process of replacing the primary eyewall by the secondary eyewall lasts a mean of 36 h (Sitkowski et al. 2011).

It should be mentioned that the P_p profile (gray curve in Figs. 2c,d) would have occurred in the absence of the V_s profile prior to the onset of the ERC. At the inception of the ERC, the addition of the developing V_s profile to the pre-existing V_p profile results in the falling P_p profile, as indicated by the gray downward-pointing arrow connecting the gray solid curve to the black, short-dashed curve in the figure.

The secondary tangential winds (V_s) are zero and the profiles are flat inside 45 and 15 km from the tropical cyclone center (Figs. 2a,b). In the respective figures, the "secondary" surface pressure drop (ΔP_s) calculated using (16) are -27 and -42 hPa, and the pressure profiles are flat inside 60 and 35 km from the center. It is indicated that as the secondary tangential wind maximum (V_{x_s}) further intensifies and slowly drifts inward (Fig. 2b), the relative flat-shaped P_s profile reduces and the central region of decreasing P_s constricts (Fig. 2b).

In hurricanes C and D, the bended profiles of P_{tot} at about 65 and 45 km from the storm center, respectively, are prominent (see upward-pointing arrows in Figs.2c,d). These features clearly result from the product of two partitioned profiles of P_p, P_s and P_e, as shown by Eq. (8). The product is responsible for creating the "kinks" in the P_{tot} profiles. These bended profiles occur just inside the radii of the well-defined, secondary tangential wind maxima.

During an ERC, a significant change in the V_c profiles causes the cyclostrophic Rossby numbers (R_c) profiles to vary, especially at the two maxima and single minimum within the saddle-shaped profiles (Figs. 2a,b). The R_c peaks occur just inside the primary and secondary RMWs.

The P_{tot} profiles (Figs. 2c,d) qualitatively resemble the isobaric height profiles observed in Hurricane David (1979; Fig. 3 of Willoughby et al. 1982). This hurricane exhibited dual-maximum concentric-eyewall tangential winds in each of the aircraft radial legs.

Wang (2009) numerically simulated the radial profiles of low-altitude tangential wind and corresponding perturbation pressure based on a series of sensitivity experiments using a cloud-resolving tropical cyclone model. The shape of our P_{tot} profile (Fig. 2d) is qualitatively similar to that of Wang's perturbation pressure profile (dot-long dashed curve in Fig. 15b, p. 1268).

4. CONCLUSIONS

A new tropical cyclone pressure-wind profile model is developed by tailoring the Wood and White (2011) parametric tangential-wind profile for tropical cyclone

applications. The simulations demonstrate that the model successfully replicates the general aspects of the observed profiles of gradient wind and surface pressure (or geopotential height) in tropical cyclones. The partitioning scheme is a useful diagnostic technique that permits investigators to quantitatively describe and interpret the significant fluctuations in central surface pressure deficits and cyclostrophic/gradient wind maxima due to evolving primary and secondary eyewalls during eyewall replacement cycles. Anticipating changes in tropical cyclone intensity due to eyewall replacement cycles is one of the most challenging aspects of tropical cyclone forecasting. The main conclusions of this study are as follows:

1. The shape velocity parameters (κ, η, λ) play a vital role in modulating all portion of the cyclostrophic/gradient wind profile. In our formulation, the wind profile is defined by (a) the κ parameter that primarily controls the inner wind profile near the storm center, (b) the η parameter that predominantly determines the outer profile, and (c) the λ parameter that mainly dictates the sharpness of the cyclostrophic/gradient wind profile spanning the wind maximum. These parameters provide enough flexibility to approximate the full range of observed tropical cyclone wind profiles.
2. The central surface pressure deficit at the storm center and the surface pressure profile are sensitive to the shape velocity parameters in the wind profile. When a single-maximum eyewall tangential wind profile evolves to a dual-maximum eyewall tangential wind profile, the surface pressure profile falls prior to the onset of an eyewall replacement cycle, even if a primary gradient wind maximum and radius of the maximum remain unchanged.
3. As an inner eyewall collapses after the inception of the cycle, the central surface pressure will increase only when the pressure rise due to the inner eyewall's deterioration is greater than the pressure fall due to the outer eyewall's continuing intensification (Willoughby et al. 1982). When the outer eyewall becomes a new inner eyewall, the central surface pressure associated with the inner eyewall continues to fall if the storm intensifies again.
4. For an intense tropical cyclone with its well-defined, dual-maximum concentric eyewall structure, a "kink" in the composite surface pressure profile stems from a product of two partitioned pressure profiles (the primary and secondary surface pressure profiles), always occurring just inside of the radii of the well-defined, secondary tangential wind maxima.

5. REFERENCES

Black, M. L., and H. E. Willoughby, 1992: The concentric eyewall cycle of Hurricane Gilbert. *Mon. Wea. Rev.,* **120,** 947-957.

Kepert, J. D., 2001: The dynamics of boundary-layer jets within the tropical cyclone core. Part I: Linear theory. *J. Atmos. Sci.,* **58,** 2469-2484.

_____, and Y. Wang, 2001: The dynamics of boundary-layer jets within the tropical cyclone core. Part II: Nonlinear enhancement. *J. Atmos. Sci.,* **58,** 2485-2501.

Knaff, J. A., and R. M. Zehr, 2007: Reexamination of tropical cyclone wind-pressure relationships. *Wea. Forecasting,* **22,** 71-88.

Marks, F. D., P. G. Black, M. T. Montgomery, and R. W. Burpee, 2008: Structure of the eye and eyewall of Hurricane Hugo (1989). *Mon. Wea. Rev.,* **136,** 1237-1259.

Press, W. H., S. A. Teukolsky, W. T. Vetterling, and B. P. Flannery, 1992: *Numerical Recipes in Fortran 77: The Art of Scientific Computing.* 2nd ed., Cambridge University, 933 pp.

Schubert, W. H., J. J. Hack, P. L. Silva Dias, and S. R. Fulton, 1980: Geostrophic adjustment in an axisymmetric vortex. *J. Atmos. Sci.,* **37,** 1464-1483.

Sitkowski, M. J. P. Kossin, and C. M. Rozoff, 2011: Intensity and structure changes during hurricane eyewall replacement cycles. *Mon. Wea. Rev.,* **139,** 3829-3847.

U.S. Standard Atmosphere, 1976, U.S. Government Printing Office, Washington, D.C., 227 pp.

Wang, Y., 2009: How do outer spiral rainbands affect tropical cyclone structure and intensity? *J. Atmos. Sci.,* **66,** 1250-1273.

Willoughby, H. E., 1990a: Temporal changes of the primary circulation in tropical cyclones. *J. Atmos. Sci.,* **47,** 242-264.

_____, 1990b: Gradient balance in tropical cyclones. *J. Atmos. Sci.,* **47,** 265-274.

_____, 1991: Reply. *J. Atmos. Sci.,* **48,** 1209-1212.

_____, 2011: The golden radius in balanced atmospheric flows. *Mon. Wea. Rev.,* **139,** 1164-1168.

_____, 1995: Mature structure and evolution. *Global Perspectives on Tropical Cyclones,* R. L. Elsberry, Ed., WMO Tech Doc. WMO/TD-No. 693, Rep. TCP-38, 21-62.

_____, and M. E. Rahn, 2004: Parametric representation of the primary hurricane vortex. Part I: Observations and evaluation of the Holland (1980) model. *Mon. Wea. Rev.,* **132,** 3033-3048.

_____, J. A. Clos, and M. G. Shoreibah, 1982: Concentric eye walls, secondary wind maxima, and the evolution of the hurricane vortex. *J. Atmos. Sci.,* **39,** 395-411.

Wood, V. T., and L. W. White, 2011: A new parametric model of vortex tangential-wind profiles: Development, testing, and verification. *J. Atmos. Sci.,* **68,** 990-1006.

Table 1. Model parameters are given which produced different radial profiles of V_i for four experiments. The subscript i represents the number of individual wind profiles [i.e., $i=1$ corresponding to p (primary) and $i=1$ corresponding to s (secondary)].

Tropical Cyclone Stage	V_{x_i} (m s^{-1})	R_{x_i} (km)	κ_i	η_i	λ_i	R_{cx_i}
Hurricane A	$V_p : 45$	15	1.0	1.5	0.20	60
Hurricane B	$\begin{cases} V_p : 45 \\ V_s : 20 \end{cases}$	15 120	1.0 3.7	1.5 3.8	0.20 0.30	60 3
Major Hurricane C	$\begin{cases} V_p : 60 \\ V_s : 30 \end{cases}$	8 70	1.5 10.0	2.0 10.4	0.13 0.05	151 9
Major Hurricane D	$\begin{cases} V_p : 30 \\ V_s : 45 \end{cases}$	8 50	1.3 4.5	1.7 5.0	0.05 0.05	75 18

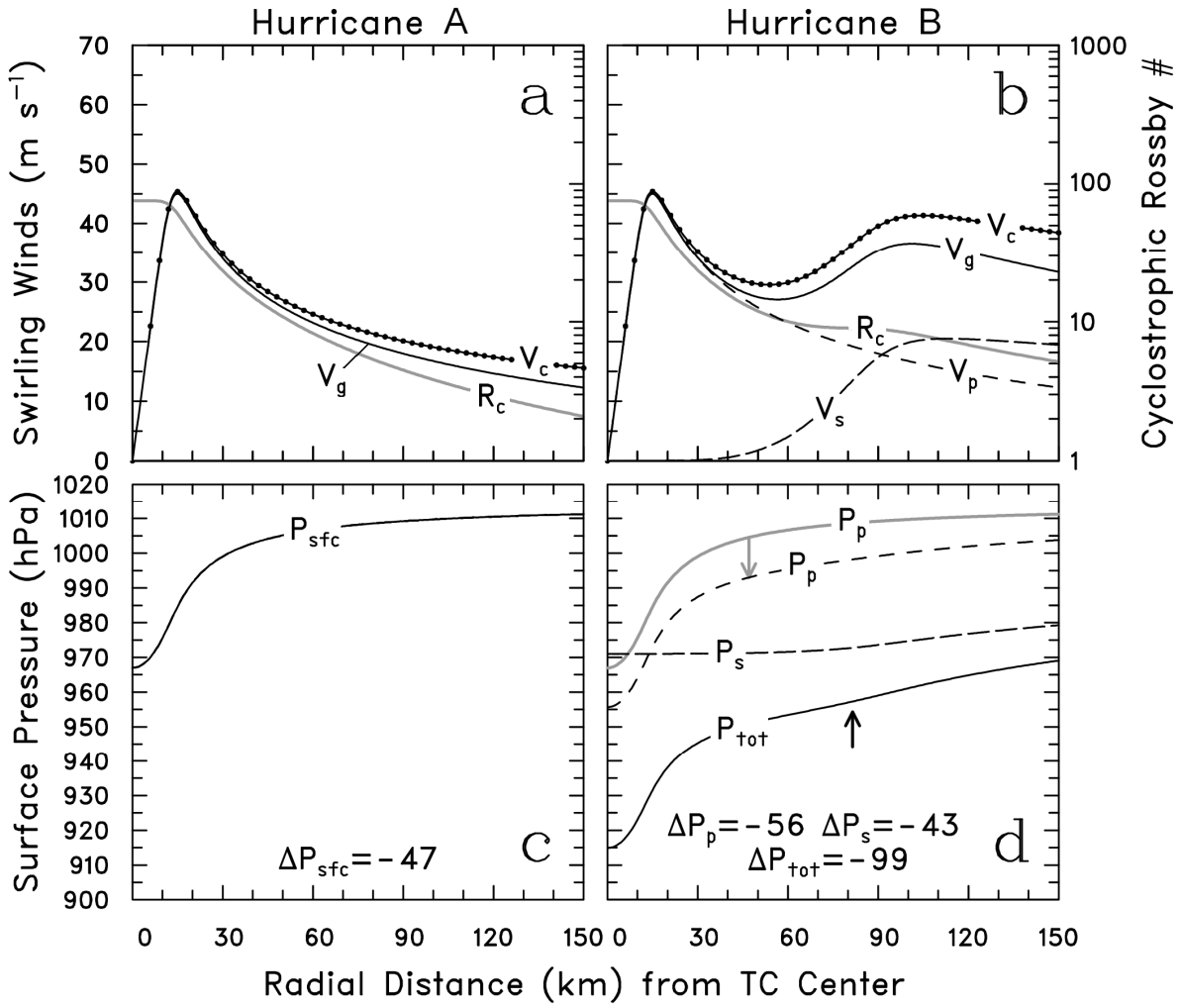

Fig. 1. Radial profiles of (a) single- and (b) dual-maximum eyewall gradient (V_g, solid curve) and cyclostrophic (V_c, dot-line curve) wind profiles for hurricanes A and B. In panels a and b, the gray curve represents the cyclostrophic Rossby number (R_c). Note that the ordinate scale on the right side of panels a and b is logarithmic. In panel b, the radial profiles of the model primary (V_p, short-dashed curve) and secondary (V_s, long-dashed curve) tangential winds are indicated. In panel d, the radial profiles of the primary (P_p, black short-dashed and gray solid curves), secondary (P_s, long-dashed curve) surface pressures, and total surface pressure ($P_{sfc} \equiv P_{tot}$, solid curve) correspond to V_p, V_s and $V_c = V_p + V_s$, respectively. The gray curve of P_p is identical to the surface pressure profile (solid curve of P_{sfc} in panel c) that hurricane B would have without the presence of the V_s profile. Arrows are discussed in text.

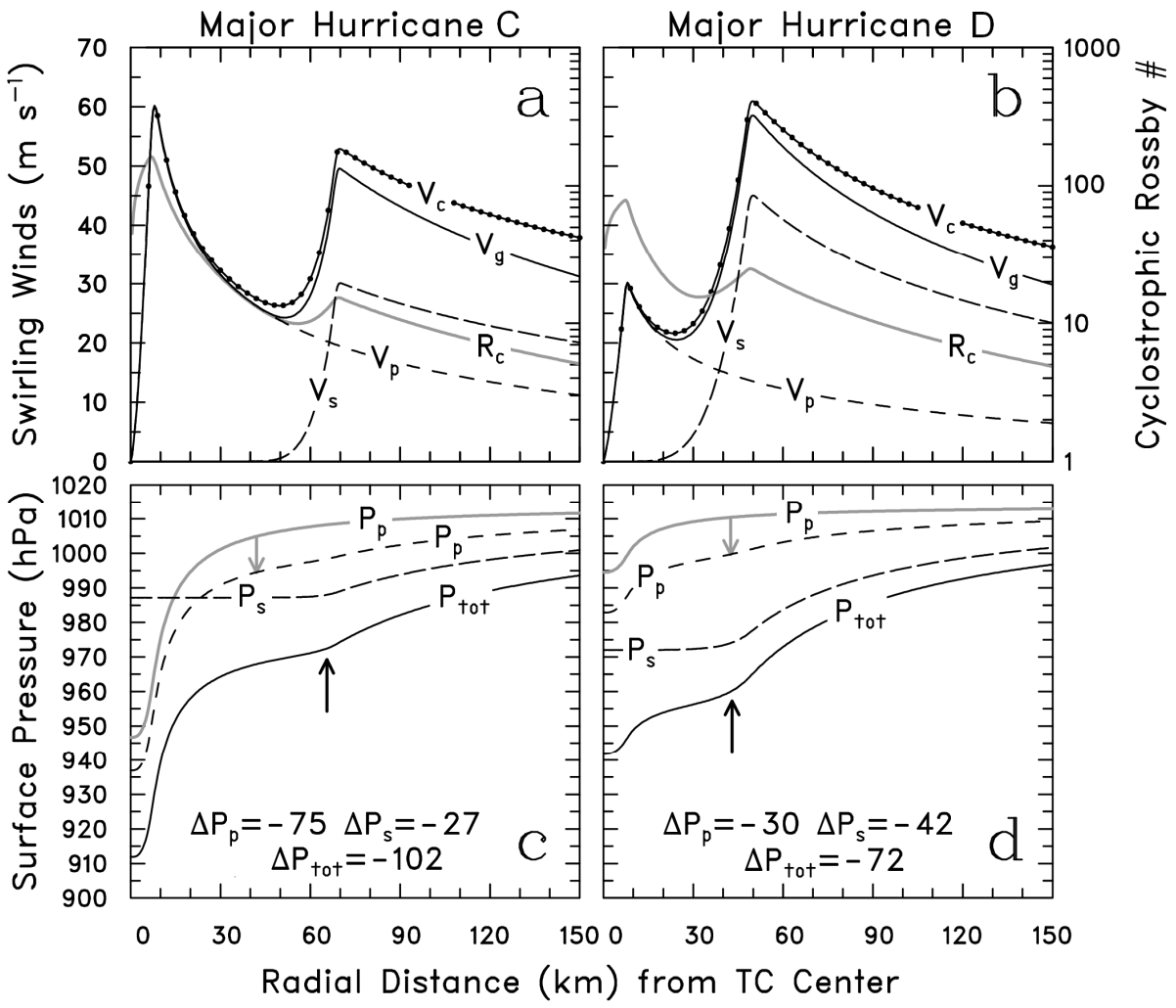

Fig. 2. Same as Fig. 1b, except for the model parameters for major hurricanes C and D are varied (see Table 1).